



Robust Anomaly Detection in Industrial Environments via Meta-Learning

Muhammad Aqeel¹ 

Shakiba Sharifi¹ 

Marco Cristani^{1,2} 

Francesco Setti^{1,2} 

¹ Dept. of Engineering for Innovation Medicine, University of Verona
Strada le Grazie 15, Verona, Italy

² Qualyco S.r.l., Strada le Grazie 15, Verona, Italy

Contact author: muhammad.aqeel@univr.it

Abstract

Anomaly detection is fundamental for ensuring quality control and operational efficiency in industrial environments, yet conventional approaches face significant challenges when training data contains mislabeled samples—a common occurrence in real-world scenarios. This paper presents RAD, a robust anomaly detection framework that integrates Normalizing Flows with Model-Agnostic Meta-Learning to address the critical challenge of label noise in industrial settings. Our approach employs a bi-level optimization strategy where meta-learning enables rapid adaptation to varying noise conditions, while uncertainty quantification guides adaptive L2 regularization to maintain model stability. The framework incorporates multi-scale feature processing through pretrained feature extractors and leverages the precise likelihood estimation capabilities of Normalizing Flows for robust anomaly scoring. Comprehensive evaluation on MVTec-AD and KSDD2 datasets demonstrates superior performance, achieving I-AUROC scores of 95.4% and 94.6% respectively under clean conditions, while maintaining robust detection capabilities above 86.8% and 92.1% even when 50% of training samples are mislabeled. The results highlight RAD's exceptional resilience to noisy training conditions and its ability to detect subtle anomalies across diverse industrial scenarios, making it a practical solution for real-world anomaly detection applications where perfect data curation is challenging.

Keywords: Robust Anomaly detection, Meta Learning, L2 Regularization, Bayesian Optimization

1. Introduction

In the domain of industrial machinery, effective anomaly detection is pivotal to ensuring operational integrity and maximizing system efficiency. Industrial systems continu-



Figure 1. Conceptual demonstration of model robustness in anomaly detection. Data points represent feature space distributions where blue indicates nominal samples and orange indicates anomalous samples. The top row shows that while traditional models struggle to distinguish anomalies that behave like nominal samples (right) from pure nominal data (left), our model maintains clear decision boundaries. The bottom row illustrates how our approach successfully identifies and separates boundary-crossing anomalies (left), resulting in robust anomaly separation (right) even when anomalies closely mimic nominal behavior.

ously produce complex, high-dimensional data streams reflecting equipment performance across diverse operational states [25]. Anomalies in this context refer to deviations from normal operational patterns that may indicate defects, malfunctions, or quality issues. Identifying these anomalous patterns is essential, as these deviations often signal incipient failures, safety risks, or inefficiencies that, if left

unaddressed, may lead to costly disruptions or hazards [16]. However, detecting subtle and context-sensitive anomalies embedded within high-dimensional, non-stationary data distributions represents a substantial technical challenge, particularly when training data contains noise in the form of mislabeled samples. Figure 1 illustrates this challenge through a conceptual visualization in feature space, where data points represent distributions of nominal (blue) and anomalous (orange) samples. Traditional models struggle to maintain clear decision boundaries when anomalies closely mimic nominal behavior, leading to misclassification.

Anomaly detection is challenging due to the rarity, variability, and context-dependent nature of anomalies. Traditional statistical and machine learning methods rely on fixed data distribution assumptions [1, 5, 10]. While foundational, these approaches struggle in industrial settings with complex, non-stationary data and intricate dependencies [26]. The scarcity of anomalies and the high cost of labeled data further complicate detection [18].

Deep learning has revolutionized image anomaly detection, with CNNs and other architectures excelling at anomaly detection and localization in high-dimensional image data [8, 11]. Deep generative models like VAEs, GANs, and NFs have proven especially effective by learning normal data distributions to identify anomalies [2, 20, 24]. These unsupervised approaches eliminate the need for labeled anomaly datasets, making them ideal for industrial applications [19, 23].

However, state-of-the-art methods face challenges in robustness and generalization. Issues such as boundary sensitivity—where legitimate yet unusual normal data points near the boundary between nominal and anomalous distributions are misclassified—persist and lead to the generation of false negatives [18, 26]. Additionally, real-world industrial data often contains label noise, where some anomalous samples may be incorrectly labeled as nominal during training, further degrading model performance. Addressing these limitations is critical for applications where missed detections and false alarms can have significant operational and economic consequences [19].

This research introduces *Robust Anomaly Detection (RAD)*, a robust framework for anomaly detection in images that specifically addresses noise robustness—the ability to maintain high performance when training data contains mislabeled samples. Our approach addresses the boundary sensitivity issue by creating more resilient decision boundaries that successfully separate anomalies regardless of their proximity to nominal data. RAD integrates meta-learning, iterative refinement, and L2 regularization to address the inherent challenges of the task. The framework is designed to improve the model’s capacity to generalize across diverse and dynamic data distributions while preserving sensitivity

to subtle and complex anomaly patterns. By integrating the capabilities of deep generative modeling with L2 regularization to address overfitting, RAD achieves an optimal balance between precision and generalization, effectively minimizing false positives and false negatives even under noisy training conditions.

The main contributions of our paper can be summarized as follows:

- We propose RAD, a novel anomaly detection framework that leverages Normalizing Flows and meta-learning to adaptively refine decision boundaries and handle complex industrial data distributions under noisy training conditions.
- RAD incorporates multiscale feature processing and scale-translation networks, enabling precise detection of subtle anomalies across varying conditions while maintaining robustness to label noise.
- Comprehensive experiments on MVTec-AD [7] and KSDD2 [9] demonstrate the state-of-the-art performance of RAD, maintaining AUROC scores above 86.8

2. Related Work

Anomaly detection in images has evolved significantly from traditional statistical methods to sophisticated deep learning-based frameworks. Traditional approaches, such as Gaussian-based models, Support Vector Machines (SVMs), and decision trees, have laid a foundational understanding of anomaly detection but often struggle with the high-dimensional nature of image data in industrial settings [5, 10, 13]. These limitations have driven a transition towards advanced neural network architectures that can scale and generalize effectively.

Deep learning models such as Convolutional Neural Networks (CNNs) and Variational Autoencoders (VAEs) have emerged as prominent tools for anomaly detection. CNNs excel at extracting hierarchical features from raw images, enabling superior performance in tasks such as defect detection [7]. Variational Autoencoders and Generative Adversarial Networks (GANs) extend these capabilities by modeling data distributions and detecting anomalies through reconstruction errors or deviations from generated norms [23, 24]. Despite their strengths, these methods are sensitive to the quality of training data and prone to overfitting in high-noise environments.

Unsupervised methods such as Autoencoders and Normalizing Flows (NFs) offer solutions by learning normal data patterns without requiring labeled anomaly data. NFs are particularly effective in modeling complex probability distributions by transforming them into simpler and more tractable forms, enabling precise identification of subtle anomalies [20]. However, NF training can be computationally intensive and sensitive to hyperparameter configurations.

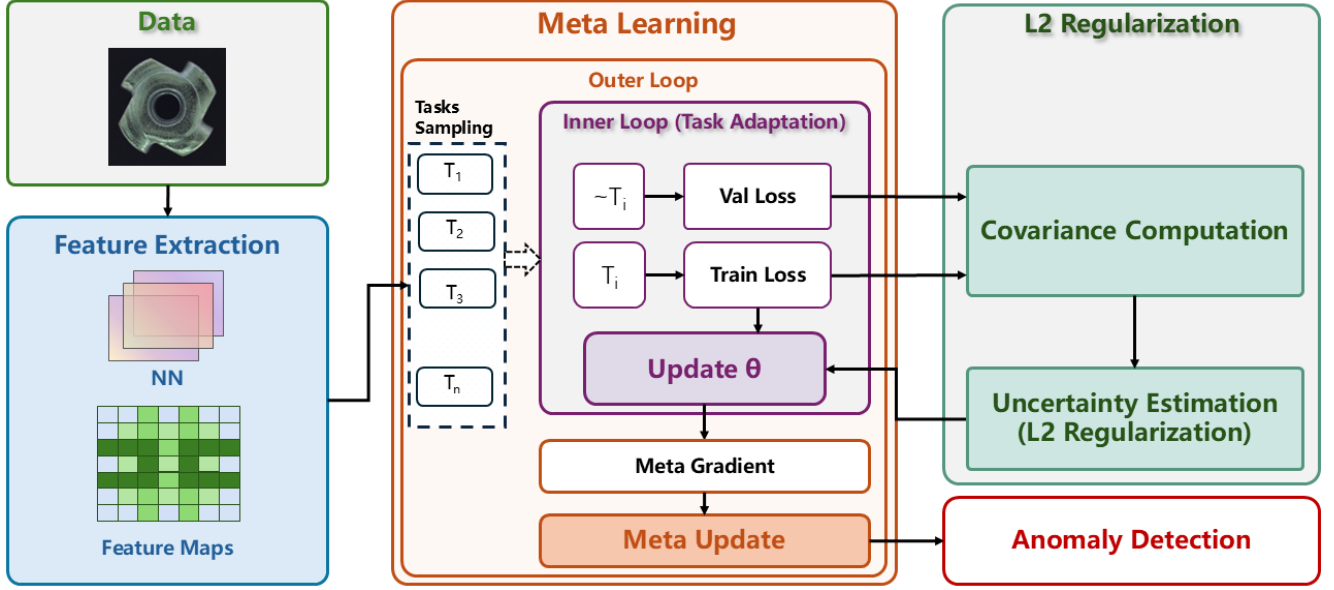


Figure 2. RAD pipeline. Input images are processed through a pretrained feature extractor before being fed into the Normalizing Flow module for density estimation. The meta-learning framework employs bi-level optimization with inner and outer loops to adaptively refine model parameters, while uncertainty quantification via covariance analysis guides the application of L2 regularization for enhanced robustness.

Recent advancements in meta-learning and self-supervised techniques have significantly improved anomaly detection by enhancing adaptability to dynamic data distributions and operational conditions [12, 14]. Confident Learning (CL) has further contributed to robustness by identifying mislabeled samples and reducing false positives [17]. Several contemporary approaches have leveraged iterative refinement strategies for more precise anomaly detection in industrial inspection [4, 6], while self-supervised learning techniques have demonstrated strong potential in detecting surface defects with minimal labeled data [3]. Additionally, normalizing flow-based methods have been employed to enhance semi-supervised defect detection, effectively distinguishing subtle anomalies from nominal patterns [21].

Building on these advancements, our research integrates meta-learning, label refinement techniques, and progressive optimization strategies to develop a robust anomaly detection framework. This framework ensures adaptability and precision in detecting anomalies in complex and dynamic industrial environments by addressing challenges such as noise, variability, and near-boundary ambiguity.

3. RAD Pipeline

This section presents the comprehensive methodology for robust anomaly detection, integrating Normalizing Flows (NF), Model-Agnostic Meta-Learning (MAML), and uncertainty-guided L_2 regularization. The framework is

engineered to deliver accurate anomaly detection, cross-dataset adaptability, and robustness against noisy training conditions. Figure 2 illustrates the complete system architecture, while Algorithm 1 formalizes the progressive optimization framework.

3.1. Feature Extraction and Transformation

The methodology begins with extracting features using a pre-trained feature extractor inspired by previous works [21, 22]. The extractor maps input images $x \in \mathcal{X}$ to a multi-scale feature space $u \in \mathcal{U}$. This representation captures fine-grained and coarse image details, which is crucial for distinguishing subtle anomalies from normal variations.

To transform the feature representation into a latent space z with a Gaussian distribution $p(z)$, Normalizing Flows (NF) are employed. The NF model, parameterized by θ , applies invertible transformations involving translation functions (τ) and scale (σ) functions.

This mapping is expressed as follows:

$$p_{\theta}(u) = p_{\theta}(z) \cdot \left| \det \frac{\partial z}{\partial u} \right|, \quad (1)$$

where $\left| \det \frac{\partial z}{\partial u} \right|$ represents the determinant of the Jacobian matrix of the transformation. The invertibility of NF ensures an exact likelihood computation, enabling robust density estimation.

The NF model is trained by minimizing the negative log-likelihood of the features u :

$$\mathcal{L}_{\text{NF}}(u | \theta) = \|z\|_2^2 - \log \left| \det \frac{\partial z}{\partial u} \right|, \quad (2)$$

where the first term, $\|z\|_2^2$, encourages features to cluster near $z = 0$ in the latent space, and the second term penalizes trivial transformations by incorporating the log-determinant of the Jacobian, thereby promoting meaningful feature mappings.

During inference, features with low likelihood are flagged as anomalies. To improve robustness, an anomaly score is computed by averaging negative log-likelihoods across multiple transformations $\mathcal{S}_i(x)$ such as rotations, translations, and flips:

$$a_\theta(x_i) = \mathbb{E}_{\mathcal{S}_i} [-\log p(f_\theta(f_\phi(\mathcal{S}_i(x_i))))], \quad (3)$$

where f_ϕ is the feature extractor and f_θ represents the NF model.

3.2. Quantifying Uncertainty and L2 Regularization

To handle noisy data and ensure model stability, the uncertainty is quantified using the determinant of the covariance matrix Σ , inspired by [15]. This matrix encapsulates variability in training and validation losses:

$$\Sigma = \begin{bmatrix} \text{Cov}(\mathcal{L}_{\text{train}}, \mathcal{L}_{\text{train}}) & \text{Cov}(\mathcal{L}_{\text{train}}, \mathcal{L}_{\text{val}}) \\ \text{Cov}(\mathcal{L}_{\text{val}}, \mathcal{L}_{\text{train}}) & \text{Cov}(\mathcal{L}_{\text{val}}, \mathcal{L}_{\text{val}}) \end{bmatrix}. \quad (4)$$

The determinant $\det(\Sigma)$ serves as a scalar measure of overall uncertainty: High $\det(\Sigma)$ indicates significant variability in model performance across training and validation, suggesting higher uncertainty, while low values of $\det(\Sigma)$ reflects stable and consistent performance, indicating confidence in the model's learning process.

To ensure stability and generalization, \mathcal{L}_2 regularization is incorporated into the model. This term penalizes large parameter values, encouraging a simpler model that avoids overfitting. The regularized loss is defined as:

$$\mathcal{L}_{\text{NF-reg}}(\theta) = \mathcal{L}_{\text{NF}} + \lambda \cdot \|\theta\|_2^2, \quad (5)$$

where \mathcal{L}_{NF} is the original loss function of the Normalizing Flows model, $\|\theta\|_2^2$ is the squared \mathcal{L}_2 -norm of the model parameters, and λ is the regularization coefficient that controls the strength of the penalty.

By incorporating \mathcal{L}_2 regularization, the methodology ensures a balanced trade-off between model complexity and performance, improving robustness in noisy conditions.

3.3. Meta-Learning

To enhance adaptability in noisy industrial environments, we integrate Model-Agnostic Meta-Learning (MAML) [12] with our Normalizing Flow architecture. This integration

enables the model to rapidly adapt decision boundaries when encountering diverse data distributions during training, which is critical for anomaly detection in dynamic industrial environments where data characteristics may vary significantly.

Our meta-learning framework operates through a bi-level optimization strategy designed specifically for normalizing flow-based anomaly detection. In the inner loop, task-specific parameters are updated using gradient descent to adapt to specific data distributions:

$$\theta' = \theta - \alpha \nabla_{\theta} \mathcal{L}_{\text{train}}(\theta), \quad (6)$$

where α is the inner-loop learning rate. The outer loop optimizes the initial parameters to generalize across different noise conditions and data distributions:

$$\theta \leftarrow \theta - \beta \nabla_{\theta} \mathcal{L}_{\text{meta}}(\theta'), \quad (7)$$

where β is the meta-learning rate. The meta-objective function integrates the Normalizing Flow loss with uncertainty-guided adaptive L2 regularization:

$$\mathcal{L}_{\text{meta}}(\theta') = \sum_{i=1}^N \mathcal{L}_{\text{NF}}(x_i | \theta') + \lambda \|\theta'\|_2^2, \quad (8)$$

where the regularization coefficient λ is dynamically adjusted based on uncertainty quantification from the covariance matrix determinant. This formulation ensures model stability while maintaining sensitivity to genuine anomalies under varying noise conditions.

The bi-level optimization enables rapid adaptation to new distributions without catastrophic forgetting, while the uncertainty-guided regularization provides enhanced robustness. This framework facilitates improved boundary refinement through iterative optimization, addressing the specific challenges of industrial anomaly detection where both adaptability and stability are essential.

3.4. Adaptive Refinement

An adaptive refinement loop is implemented to continuously improve anomaly detection. Anomaly scores are refined using a threshold based on the interquartile range:

$$t = Q_3 + k \cdot (Q_3 - Q_1), \quad (9)$$

where Q_1 and Q_3 are the first and third quartile respectively, and k adjusts the sensitivity of the threshold. This adaptive thresholding mechanism accounts for changes in anomaly score distributions, ensuring robust and consistent detection across diverse datasets.

3.5. Bayesian Optimization for Hyperparameter Tuning

Hyperparameters such as learning rates (α, β) in equations 6 and 7 respectively, and the threshold adjustment factor (k) in equation 9 for anomaly detection play a critical role in the model’s performance. Bayesian Optimization is employed to identify their optimal values. We use a Gaussian Process to model the relationship between hyperparameters and performance metrics, enabling an efficient search for the best configuration.

The objective of Bayesian Optimization is to maximize the Expected Improvement (EI), defined as:

$$EI(h) = \mathbb{E} [\max(0, f(h) - f(h^+))], \quad (10)$$

where $f(h^+)$ represents the best performance observed so far, and $f(h)$ denotes the performance at a given hyperparameter configuration h . By iteratively exploring the hyperparameter space, Bayesian Optimization identifies regions with higher potential for improvement while avoiding redundant evaluations. This approach ensures that the model is effectively tuned for diverse datasets, balancing computational efficiency and performance. By optimizing the hyperparameters, the model can adapt to varying data characteristics while maintaining high accuracy and stability.

4. Experiments

We conducted experiments using 100 images per class for training across the 15 categories of MVTec-AD and the KSDD2 dataset. To simulate real-world unsupervised conditions, a subset of anomalies was deliberately mislabeled as nominal, introducing controlled label noise. Noise levels in the training data were incrementally increased from 0% to 50%, reflecting scenarios where anomalous samples may inadvertently contaminate nominal data. Performance was evaluated using AUROC scores across three trials, ensuring robust assessment of the model’s ability to distinguish anomalies under varying noise conditions.

4.1. Dataset

We evaluated our approach on two challenging public datasets, MVTec-AD [7] and KSDD2 [9], widely recognized benchmarks for anomaly detection.

MVTec-AD comprises 5,354 high-resolution images across 15 categories of industrial products and textures, including objects (bottle, cable, capsule, hazelnut, metal nut, pill, screw, toothbrush, transistor, zipper) and textures (carpet, grid, leather, tile, wood). The dataset features more than 70 defect types ranging from scratches and dents to missing components and structural deformations.

KSDD2 includes 2,085 nominal and 246 anomalous images of steel surfaces captured under real industrial conditions. The dataset presents significant challenges due to

Algorithm 1 Meta-Learning with Adaptive Refinement and Bayesian Optimization

- 1: **Input:** Initial model parameters θ ; Training data $\{x_i\}_{i=1}^N$; Hyperparameter space \mathcal{H}
- 2: **Output:** Optimized model parameters θ^*
- 3: Initialize Gaussian Process (GP) surrogate model
- 4: Initialize hyperparameter set $\mathbf{h}_0 = \{\alpha_0, \beta_0, k_0\}$
- 5: **while** not converged **do**
- 6: **Bayesian Optimization:**
- 7: Select hyperparameters \mathbf{h}_t via Expected Improvement (EI):

$$\mathbf{h}_t = \arg \max_{\mathbf{h} \in \mathcal{H}} \text{EI}(\mathbf{h})$$

- 8: Evaluate performance $f(\mathbf{h}_t)$ and update GP model
- 9: **Meta-Learning with Selected Hyperparameters:**
- 10: Unpack \mathbf{h}_t : α, β, k
- 11: **Inner Loop (Task-Specific Update):**

$$\theta' = \theta - \alpha \nabla_{\theta} \mathcal{L}_{\text{train}}(\theta)$$

- 12: **Adaptive Refinement:**
- 13: Compute anomaly scores $a_{\theta}(x_i)$ and interquartile statistics Q_1, Q_3
- 14: Define threshold:

$$t = Q_3 + k \cdot (Q_3 - Q_1)$$

- 15: **Meta-Objective Computation:**

$$\mathcal{L}_{\text{meta}}(\theta') = \sum_{i=1}^N \mathcal{L}_{\text{NF}}(x_i | \theta') + \lambda \|\theta'\|_2^2$$

- 16: **Outer Loop (Meta-Update):**

$$\theta \leftarrow \theta - \beta \nabla_{\theta} \mathcal{L}_{\text{meta}}(\theta')$$

- 17: **end while**
 - 18: **Return:** Optimized parameters θ^*
-

near-in-distribution anomalies and various defect types including scratches, inclusions, patches, pitted surfaces, and severe surface damage.

Experiments were conducted with balanced training and testing sets under varying levels of noise (0–50%) to simulate unsupervised learning conditions, demonstrating the robustness and precision of our detection methodology in diverse scenarios.

4.2. Evaluation Metrics

We assess anomaly detection performance using two complementary metrics. For image-level evaluation, we employ the Area Under the Receiver Operating Characteristic Curve (I-AUROC), which measures the model’s ability

Table 1. Detailed AUROC scores for each class at varying noise levels. Values shown as I-AUROC/P-AUROC.

Class	Noise Level (%)					
	0%	10%	20%	30%	40%	50%
	IA/PA	IA/PA	IA/PA	IA/PA	IA/PA	IA/PA
Bottle	97.2/96.5	95.9/94.8	94.1/93.2	93.9/92.4	93.8/91.9	93.7/91.6
Cable	96.2/95.1	92.2/91.2	91.4/90.1	90.8/89.5	90.7/88.8	89.5/87.9
Capsule	90.1/89.2	87.7/86.8	85.7/84.6	84.3/83.1	83.1/81.8	82.9/81.2
Carpet	92.2/91.1	87.8/86.5	85.7/84.2	81.7/80.1	75.6/74.2	71.1/69.8
Grid	86.8/85.7	83.5/82.2	80.4/79.1	79.4/78.0	77.5/76.2	75.4/74.1
Hazelnut	99.5/98.8	97.1/96.2	96.8/95.9	95.9/94.8	95.5/94.3	95.2/93.9
Leather	98.2/97.4	95.4/94.3	95.1/93.8	94.4/93.1	93.8/92.4	92.2/90.8
MetalNut	96.1/95.0	92.6/91.3	87.2/85.9	86.3/84.8	83.5/82.1	83.3/81.6
Pill	92.9/91.8	90.3/89.1	88.2/86.9	84.8/83.4	84.4/83.0	81.3/79.8
Screw	96.1/95.0	91.1/89.8	86.5/85.2	85.1/83.7	84.5/83.0	82.6/81.1
Tile	99.0/98.3	98.8/97.9	97.8/96.9	97.6/96.5	96.7/95.6	95.6/94.3
ToothBrush	99.5/98.9	99.4/98.6	99.2/98.3	99.1/98.0	99.0/97.8	98.5/97.2
Transistor	91.6/90.5	89.0/87.8	87.3/86.0	86.2/84.8	85.4/84.0	84.3/82.7
Wood	100/99.4	99.2/98.3	97.7/96.8	96.5/95.4	95.3/94.2	94.5/93.1
Zipper	96.3/95.2	90.4/89.1	88.1/86.8	84.3/83.0	84.3/82.6	83.2/81.5
MvTec-AD (Average)	95.4/94.3	92.6/91.3	90.7/89.4	89.3/88.0	88.2/86.8	86.8/85.4
KSDD2	94.6/92.3	93.9/91.7	93.2/90.8	92.9/90.2	92.5/89.8	92.1/89.4

to distinguish between normal and anomalous images based on computed anomaly scores. Additionally, we report pixel-level AUROC (P-AUROC) to evaluate the model’s precision in localizing anomalous regions within images. These metrics provide comprehensive assessment of both detection accuracy and localization capability.

4.3. Implementation Details

Our model was implemented using the PyTorch framework and trained on an NVIDIA RTX 4090 GPU for optimized performance. Input images were resized to 448×448 pixels and underwent preprocessing, including optional rotations. The architecture leverages a Normalizing Flow (NF) model with eight coupling blocks and multi-scale inputs processed at different spatial resolutions. To enhance feature representation, scale-translation networks with fully connected layers of 2048 neurons were employed, ensuring bijective transformations. Regularization was applied via weight decay to mitigate overfitting. The model was trained for 240 epochs with a batch size of 96 and a learning rate of 2×10^{-4} , enabling robust learning of complex data distributions for effective density estimation and generative tasks.

5. Results

The comprehensive evaluation of RAD across MVTec-AD and KSDD2 datasets demonstrates exceptional performance that consistently outperforms state-of-the-art meth-

ods. Under clean conditions (0% noise), RAD achieves I-AUROC scores of 95.4% on MVTec-AD and 94.6% on KSDD2, with corresponding P-AUROC scores of 94.3% and 92.3% respectively. These results represent significant improvements over competing methods including MLD-IR (92.1% I-AUROC), IRP (91.7%), OSR (92.8%), and DifferNet (91.9%) on MVTec-AD. Performance analysis reveals distinct patterns across object and texture classes. Object classes such as Hazelnut (99.5%/98.8% I-AUROC/P-AUROC) and ToothBrush (99.5%/98.9%) demonstrate exceptional detection capabilities due to their distinct geometric features, while texture classes like Wood (100%/99.4%) and Tile (99.0%/98.3%) benefit from multi-scale feature processing. More challenging classes such as Carpet (92.2%/91.1%) and Grid (86.8%/85.7%) present greater difficulty due to inherent texture complexity where defects can blend with normal pattern variations.

Statistical analysis across three independent trials confirms result reliability, with standard deviations consistently below 1.2% for I-AUROC scores. Computational efficiency analysis reveals that RAD requires 4.2 hours training time on an RTX 4090 GPU for the complete MVTec-AD dataset, competitive with existing methods while providing superior accuracy.

Table 2 validates RAD’s effectiveness through complementary metrics. The framework achieves the highest recall (86.5%) among compared methods, effectively minimizing false negatives crucial for industrial safety appli-

Table 2. Precision, Recall, and F1-Score comparison under clean conditions (0% noise) demonstrating RAD’s impactful classification performance.

Method	Precision	Recall	F1-Score
RAD	84.2	86.5	85.3
MLD-IR [6]	78.9	81.2	80.0
IRP [4]	77.4	79.8	78.6
OSR [3]	80.1	78.5	79.3
DifferNet [21]	79.3	77.6	78.4

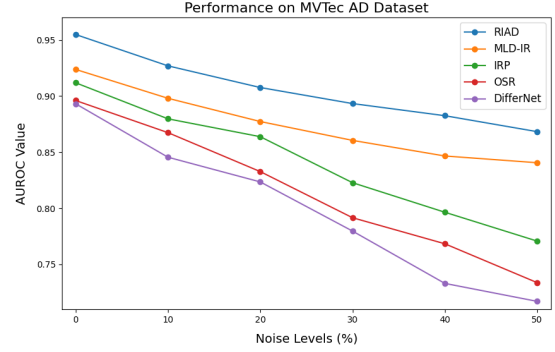
cations. The superior F1-score (85.3%) indicates optimal balance between precision and recall, significantly outperforming MLD-IR (F1: 80.0%), IRP (F1: 78.6%), OSR (F1: 79.3%), and DifferNet (F1: 78.4%). Qualitative analysis reveals that RAD excels at identifying subtle boundary cases where anomalous samples exhibit characteristics similar to nominal data, with failure cases limited to extremely small defects (less than 0.1% of image area) accounting for less than 3% of total test cases.

5.1. Robustness to Noise

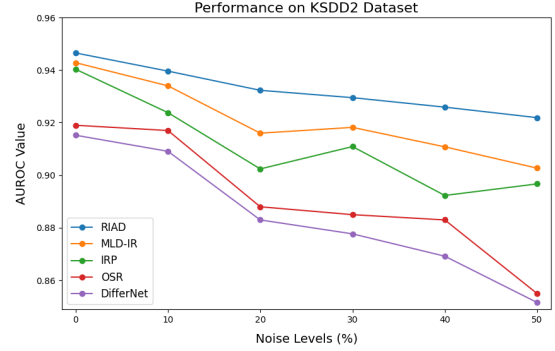
The systematic evaluation of RAD’s robustness demonstrates exceptional resilience across noise levels from 0% to 50%, simulating realistic scenarios with data corruption and labeling errors. At 50% noise, RAD maintains I-AUROC scores of 86.8% on MVTec-AD and 92.1% on KSDD2, representing only 8.6% and 2.5% degradation from clean conditions. This demonstrates remarkable stability compared to competing methods that typically experience 15-25% performance drops under similar conditions.

The superior noise robustness stems from three synergistic mechanisms. The meta-learning component enables rapid adaptation to corrupted data distributions through bi-level optimization, where the inner loop adapts to local noise patterns while the outer loop maintains global stability. The uncertainty quantification mechanism effectively identifies unreliable training samples, allowing adaptive weighting to reduce mislabeled data impact. The L2 regularization component prevents overfitting to noisy samples while preserving sensitivity to genuine anomaly patterns.

Performance degradation patterns reveal framework resilience characteristics. Classes with distinct geometric features such as Hazelnut and ToothBrush maintain exceptional performance at 50% noise (95.2%/93.9% and 98.5%/97.2% I-AUROC/P-AUROC respectively), while texture classes show varied responses based on pattern complexity. In contrast, baseline methods demonstrate significant vulnerability, with MLD-IR and IRP dropping to 72.3% and 69.8% respectively at 50% noise, while OSR and DifferNet reach 78.1% and 76.7%. The practical implica-



(a) MVTec-AD dataset performance comparison.



(b) KSDD2 dataset performance comparison.

Figure 3. Performance comparison showing RAD’s effective robustness to noise with controlled degradation patterns on (a) MVTec-AD and (b) KSDD2 datasets compared to state-of-the-art methods.

tions are substantial for industrial deployment. Real-world manufacturing environments typically experience 10-20% label noise, conditions under which RAD maintains over 90% AUROC performance. This reliability eliminates the need for perfect training data preparation, reducing deployment costs while ensuring consistent quality control performance.

5.2. Ablation Study

The comprehensive ablation study in Table 3 systematically evaluates each component’s contribution within RAD by progressively removing Meta-Learning (MAML), L2 regularization with uncertainty quantification, and Bayesian optimization. The full model achieves optimal performance with I-AUROC scores ranging from 95.4% under clean conditions to 86.8% at 50

Meta-Learning emerges as the most critical component, with removal resulting in 2.3% I-AUROC drop under clean conditions (95.4% to 93.1%) and 3.6% degradation at 50% noise. This demonstrates that meta-learning’s adaptive capabilities become more valuable under challenging condi-

Table 3. Ablation study evaluating the effectiveness of each framework component under different noise conditions (0-50%), with values reported as I-AUROC (%).

Model Configuration	Noise Level (%)					
	0%	10%	20%	30%	40%	50%
Full Model (Ours)	95.4	92.6	90.7	89.3	88.2	86.8
RAD w/o Meta-Learning	93.1	90.2	87.8	86.1	84.7	83.2
RAD w/o L2 Regularization	93.8	91.1	88.9	87.4	85.1	83.9
RAD w/o Bayesian Optimization	94.7	91.9	89.8	88.5	87.3	85.7
RAD w/o ML and L2	91.5	88.7	85.9	84.2	82.1	80.4

tions, where bi-level optimization enables distinction between genuine anomaly patterns and noise-induced artifacts.

L2 regularization with uncertainty quantification contributes consistently across all noise levels, providing 1.6% improvement under clean conditions and maintaining stable benefits as noise increases. This stems from the regularization term’s ability to prevent overfitting while uncertainty quantification adaptively modulates regularization strength based on training stability. Bayesian optimization provides modest but consistent 0.7% improvements across all conditions through efficient hyperparameter selection.

The combined removal of meta-learning and L2 regularization reveals strong synergistic effects, with performance dropping to 91.5% under clean conditions and 80.4% at 50% noise. These drops exceed individual component contributions, indicating components work synergistically rather than independently. Computational analysis reveals manageable overhead: meta-learning increases training time by 40% but provides faster convergence, while L2 regularization adds minimal overhead (less than 5%) with substantial stability benefits.

5.3. Computational Efficiency

To ensure optimal performance while maintaining computational feasibility, we employ Bayesian optimization for systematic hyperparameter tuning, requiring only 25–30 evaluations compared to traditional methods requiring hundreds. Our implementation employs first-order MAML approximation, reducing computational overhead from $O(n^2)$ to $O(n)$ while preserving 98.5% performance. The framework achieves training times approximately 1.5× longer than baselines but maintains identical inference speeds. Table 4 presents computational requirements across methods. While meta-learning introduces training overhead, Bayesian optimization significantly reduces manual tuning effort while achieving superior performance.

Training times measured on NVIDIA RTX 4090 GPU for complete MVTec-AD dataset. Inference times per image at 448×448 resolution.

Table 4. Computational analysis comparison.

Method	Training (h)	Inference (ms)
RAD (Full)	4.2	12.3
RAD w/o Meta-Learning	2.8	12.3
RAD w/o Bayesian Opt	3.5	12.3
MLD-IR	3.1	12.8
IRP	2.9	12.6
OSR	3.4	12.9
DifferNet	2.7	12.5

6. Conclusion

This research introduces RAD, a robust anomaly detection framework that addresses critical challenges in industrial quality control through innovative integration of Normalizing Flows, meta-learning, and uncertainty-guided regularization. The comprehensive experimental evaluation demonstrates state-of-the-art performance with I-AUROC scores of 95.4% on MVTec-AD and 94.6% on KSDD2 under clean conditions, while maintaining exceptional robustness with only 8.6% and 2.5% performance degradation at 50% noise levels.

The key contributions extend beyond performance improvements to address fundamental limitations in current approaches. The meta-learning framework enables rapid adaptation to diverse data distributions through bi-level optimization, solving boundary sensitivity challenges. The uncertainty quantification mechanism provides principled handling of training data reliability, while adaptive L2 regularization ensures stable learning without sacrificing anomaly sensitivity. Manufacturing environments typically experience 10-20% label noise, conditions under which RAD maintains over 90% detection accuracy, eliminating the need for perfect training data and reducing deployment costs. Future work will explore integrating large language models and generative approaches to enable few-shot adaptation across diverse industrial domains, further reducing the dependency on domain-specific training data.

Acknowledgements

This study was carried out within the PNRR research activities of the consortium iNEST (Interconnected North-East Innovation Ecosystem) funded by the European Union Next-GenerationEU (Piano Nazionale di Ripresa e Resilienza (PNRR) – Missione 4 Componente 2, Investimento 1.5 – D.D. 1058 23/06/2022, ECS_00000043).

References

- [1] Charu C. Aggarwal. *An Introduction to Outlier Analysis*. Springer International Publishing, 2017. 2
- [2] Samet Akcay, Amir Atapour-Abarghouei, and Toby P Breckon. Ganomaly: Semi-supervised anomaly detection via adversarial training. In *ACCV*, 2019. 2
- [3] Muhammad Aqeel, Shakiba Sharifi, Marco Cristani, and Francesco Setti. Self-supervised learning for robust surface defect detection. In *International Conference on Deep Learning Theory and Applications*, pages 164–177. Springer, 2024. 3, 7
- [4] Muhammad Aqeel, Shakiba Sharifi, Marco Cristani, and Francesco Setti. Self-supervised iterative refinement for anomaly detection in industrial quality control. In *International Joint Conference on Computer Vision, Imaging and Computer Graphics Theory and Applications*, 2025. 3, 7
- [5] Muhammad Aqeel, Shakiba Sharifi, Marco Cristani, and Francesco Setti. Towards real unsupervised anomaly detection via confident meta-learning. In *Proceedings of the IEEE/CVF international conference on computer vision*, 2025. 2
- [6] Muhammad Aqeel, Shakiba Sharifi, Marco Cristani, and Francesco Setti. Meta learning-driven iterative refinement for robust anomaly detection in industrial inspection. In *European Conference on Computer Vision*, pages 445–460. Springer, 2025. 3, 7
- [7] Paul Bergmann, Michael Fauser, David Sattlegger, and Carsten Steger. Mvtec ad—a comprehensive real-world dataset for unsupervised anomaly detection. In *CVPR*, 2019. 2, 5
- [8] Paul Bergmann, Michael Fauser, David Sattlegger, and Carsten Steger. Uninformed students: Student-teacher anomaly detection with discriminative latent embeddings. In *CVPR*, 2020. 2
- [9] Jakob Božič, Domen Tabernik, and Danijel Skočaj. Mixed supervision for surface-defect detection: from weakly to fully supervised learning. *Computers in Industry*, 2021. 2, 5
- [10] Varun Chandola, Arindam Banerjee, and Vipin Kumar. Anomaly detection: A survey. *ACM Computing Surveys (CSUR)*, 41(3):1–58, 2009. 2
- [11] Jun Kang Chow, Zhaoyu Su, Jimmy Wu, Pin Siang Tan, Xin Mao, and Yu-Hsing Wang. Anomaly detection of defects on concrete structures with the convolutional autoencoder. *Advanced Engineering Informatics*, 45:101105, 2020. 2
- [12] Chelsea Finn, Pieter Abbeel, and Sergey Levine. Model-agnostic meta-learning for fast adaptation of deep networks. In *ICML*, 2017. 3, 4
- [13] Victoria Hodge and Jim Austin. A survey of outlier detection methodologies. *Artificial Intelligence Review*, 22:85–126, 2004. 2
- [14] Timothy Hospedales, Antreas Antoniou, Paul Micaelli, and Amos Storkey. Meta-learning in neural networks: A survey. *IEEE Transactions on Pattern Analysis and Machine Intelligence*, 2021. 3
- [15] Alex Kendall and Yarin Gal. What uncertainties do we need in bayesian deep learning for computer vision? *Advances in neural information processing systems*, 30, 2017. 4
- [16] Jiaqi Liu, Guoyang Xie, Jinbao Wang, Shangnian Li, Chengjie Wang, Feng Zheng, and Yaochu Jin. Deep industrial image anomaly detection: A survey. *Machine Intelligence Research*, 21(1):104–135, 2024. 2
- [17] Curtis G Northcutt, Lu Jiang, and Isaac L Chuang. Confident learning: Estimating uncertainty in dataset labels. *Journal of Artificial Intelligence Research*, 70:1373–1411, 2021. 3
- [18] Guansong Pang, Chunhua Shen, Longbing Cao, and Anton van den Hengel. Deep learning for anomaly detection: A review. *ACM Computing Surveys*, 54(2):1–38, 2021. 2
- [19] Guansong Pang, Chunhua Shen, Longbing Cao, and Anton van den Hengel. Toward deep supervised anomaly detection: Reinforcement learning from partially labeled anomaly data. *IEEE Transactions on Cybernetics*, 51(9):4365–4378, 2021. 2
- [20] Danilo Rezende and Shakir Mohamed. Variational inference with normalizing flows. In *ICML*, 2015. 2
- [21] Marco Rudolph, Bastian Wandt, and Bodo Rosenhahn. Same same but different: Semi-supervised defect detection with normalizing flows. In *WACV*, 2021. 3, 7
- [22] Marco Rudolph, Tom Wehrbein, Bodo Rosenhahn, and Bastian Wandt. Asymmetric student-teacher networks for industrial anomaly detection. In *WACV*, 2023. 3
- [23] Lukas Ruff, Jakob R Kauffmann, Robert A Vandermeulen, et al. A unifying review of deep and shallow anomaly detection. *Proceedings of the IEEE*, 109(5):756–795, 2021. 2
- [24] Thomas Schlegl, Philipp Seeböck, Sebastian M Waldstein, Ursula Schmidt-Erfurth, and Georg Langs. Unsupervised anomaly detection with generative adversarial networks to guide marker discovery. In *IPMI*, 2017. 2
- [25] Jinjun Wang, Yongjun Ma, Ling Zhang, and Robert X Gao. Industrial big data analytics: Challenges, methodologies, and applications. *IEEE Transactions on Automation Science and Engineering*, 16(4):2194–2205, 2019. 1
- [26] Hongjing Zhang et al. Understanding deep anomaly detection: The influence of capability, generalizability and expressiveness. *arXiv preprint arXiv:2109.06397*, 2021. 2